

# Electron-phonon scattering in topological insulators

Sébastien Giraud and Reinhold Egger

*Institut für Theoretische Physik, Heinrich-Heine-Universität, D-40225 Düsseldorf, Germany*

(Received 1 March 2011; revised manuscript received 29 May 2011; published 29 June 2011)

We formulate and apply a theory of electron-phonon interactions for the surface state of a strong topological insulator. Phonons are modeled using an isotropic elastic continuum theory with stress-free boundary conditions and interact with the Dirac surface fermions via the deformation potential. We discuss the temperature dependence of the quasiparticle lifetime in photoemission and of the surface resistivity.

DOI: [10.1103/PhysRevB.83.245322](https://doi.org/10.1103/PhysRevB.83.245322)

PACS number(s): 73.20.-r, 63.20.kd, 72.10.Di

## I. INTRODUCTION

One of the presently most active areas in physics is concerned with strong topological insulator (TI) materials.<sup>1,2</sup> In these systems strong spin-orbit couplings cause band inversion and a nontrivial topology of the map from momentum to Hilbert space.<sup>3,4</sup> In a TI, as long as time-reversal invariance remains unbroken, an odd number of massless surface Dirac fermion modes is guaranteed despite the presence of a bulk gap  $\Delta_b$ . The existence of metallic two-dimensional (2D) Dirac surface states has been convincingly established using angle-resolved photoemission spectroscopy (ARPES) in bismuth selenides.<sup>1,5</sup> Typical reference materials are  $\text{Bi}_2\text{Te}_3$  or  $\text{Bi}_2\text{Se}_3$ , where  $\Delta_b \simeq 0.3$  eV allows one to observe these phenomena even at room temperature, but other material classes have also been predicted to possess a TI phase.<sup>1</sup> Attempts to observe electronic transport signatures of the surface state were only partially successful<sup>6–8</sup> since surface effects are easily masked by defect-induced residual bulk charge carriers. Anticipating progress in achieving better purity, it is important to understand what intrinsically limits the surface conductivity and the integrity of surface quasiparticles. Noting that the large and anisotropic static dielectric constant [ $\epsilon \approx 50$ –200 (Ref. 9)] implies a drastic reduction of direct Coulomb forces or charged impurity potentials, we here analyze consequences of the *electron-phonon coupling* on the TI surface state.

We focus on long-wavelength acoustic phonons which dominate the physics at low energy scales. Previous work on the thermoelectric properties of  $\text{Bi}_2\text{Te}_3$  has demonstrated that despite the quintuple-layer crystal structure, bulk acoustic phonons are reasonably well described as isotropic elastic continuum,<sup>10,11</sup> where the two Lamé parameters of the theory determine the longitudinal and transverse sound velocities,  $c_l \simeq 2800$  m/s and  $c_t \simeq 1600$  m/s, respectively. Low-temperature electronic transport is then limited by the deformation potential coupling to acoustic phonons, since piezoelectric couplings are suppressed by inversion symmetry.<sup>11</sup> TI experiments have so far only addressed the coupling to optical phonons,<sup>9,12</sup> cf. also studies for Bi surfaces.<sup>13</sup> However, massless 2D Dirac fermions are realized in graphene monolayers as well, where both theory<sup>14,15</sup> and experiment<sup>16</sup> have reported consistent results for the temperature ( $T$ ) dependence of the resistivity ( $\rho$ ): for  $T \ll T_{\text{BG}}$  (with the Bloch-Grüneisen temperature  $T_{\text{BG}} \equiv 2\hbar k_F c_s / k_B$ , Fermi momentum  $k_F$ , and sound velocity  $c_s$ ), a  $\rho \sim T^4$  scaling is found, while  $\rho \sim T$  for  $T \gg T_{\text{BG}}$ . Note that for a 2D electron gas with parabolic

dispersion and dominant deformation potential coupling, one expects  $\rho \sim T^7$  for  $T \ll T_{\text{BG}}$ .<sup>17</sup> Below, we shall discuss in detail the  $\rho(T)$  dependence of the TI surface state due to coupling to acoustic phonons. In addition, phonons are expected to cause quasiparticle decay. This implies, e.g., a finite ARPES linewidth,<sup>18,19</sup> where an anomalous behavior was observed in  $\text{Bi}_2\text{Se}_3$ .<sup>20</sup>

In this paper, we formulate and study an analytically tractable effective low-energy theory for the TI surface state coupled to acoustic phonons. The phonon modes are obtained from isotropic elastic continuum theory in a half-space with stress-free boundary conditions.<sup>21,22</sup> Their coupling to the surface fermions is predominantly via the deformation potential.<sup>23</sup> For concrete numbers, we use published<sup>10,11,24</sup> values for  $\text{Bi}_2\text{Te}_3$ . We compute the quasiparticle decay rate  $\Gamma$  and find  $\Gamma \sim T$  at high temperatures. This prediction should be observable by ARPES. Phonons also affect the surface resistivity and yield a characteristic  $T$ -dependent contribution to  $\rho$ . Our theory is flexible enough to allow for the use of microscopically derived phonon modes and coupling matrix elements, e.g., resulting from (future) numerical force-constant calculations.

## II. MODEL

We consider energies below the TI bulk gap where only surface electronic states are relevant. For the half-space  $z > 0$ , the surface-state wave function  $\chi(z)$  follows from the low-energy band structure with Dirichlet boundary conditions at  $z = 0$ ,<sup>25</sup>

$$\chi(z) = \mathcal{N}(e^{-\eta_- z} - e^{-\eta_+ z}), \quad \eta_{\pm} = \frac{B_0 \pm \sqrt{B_0^2 + 4M_0 M_1}}{2M_1}, \quad (1)$$

with normalization  $\mathcal{N}$  and material parameters ( $B_0, M_0, M_1$ ) specified in Ref. 24. Since  $M_0 M_1 < 0$  and  $B_0 / M_1 > 0$ , we have  $\text{Re}(\eta_{\pm}) > 0$  and the state (1) decays exponentially. One arrives at a massless 2D Dirac Hamiltonian (we set  $\hbar = 1$ ),<sup>1</sup>

$$H_e = \sum_{k,s=\pm} \epsilon_{ks} c_{ks}^{\dagger} c_{ks}, \quad \epsilon_{ks} = s v_F |\mathbf{k}| - \mu, \quad (2)$$

with the Fermi velocity  $v_F \simeq 4.36 \times 10^5$  m/s and the chemical potential  $\mu$  defining  $k_F = |\mu| / v_F$ . A helical eigenstate with

helicity  $s = \pm$  has its spin structure tied to the surface momentum  $\mathbf{k} = (k_x, k_y)$ . Helical fermions,  $c_{\mathbf{k}} = (c_{k+}, c_{k-})^T$ , are connected to the usual spinful operators,  $d_{\mathbf{k}} = (d_{k\uparrow}, d_{k\downarrow})^T$ , by a unitary transformation,

$$c_{\mathbf{k}} = U_{\mathbf{k}} d_{\mathbf{k}}, \quad U_{\mathbf{k}} = \frac{1}{\sqrt{2}} \begin{pmatrix} e^{i\theta_{\mathbf{k}}/2} & i e^{-i\theta_{\mathbf{k}}/2} \\ e^{i\theta_{\mathbf{k}}/2} & -i e^{-i\theta_{\mathbf{k}}/2} \end{pmatrix}, \quad (3)$$

where  $\tan \theta_{\mathbf{k}} = k_y/k_x$ .

In order to describe noninteracting acoustic phonons we employ isotropic elastic continuum theory with stress-free boundary conditions at  $z = 0$ . We briefly summarize the resulting eigenmodes<sup>21,22</sup> before turning to the electron-phonon coupling. Following the notation in Ref. 22 we label the modes by the quantum numbers  $\Lambda = (\mathbf{q}, \Omega, \lambda)$ , with surface momentum  $\mathbf{q} = (q_x, q_y)$ , frequency  $\Omega > 0$ , and mode type  $\lambda \in (H, T, L, R)$  explained below. In this nonstandard but very convenient notation, the frequency  $\Omega = \Omega_{\Lambda}$  is not specified in terms of  $\mathbf{q}$  and  $\lambda$  but represents a free parameter. With  $\mathbf{r} = (x, y)$  and surface area  $\mathcal{A}$ , the displacement field operator takes the form

$$\mathbf{U}(\mathbf{r}, z, t) = \sum_{\Lambda} \frac{1}{\sqrt{2\rho_M \mathcal{A} \Omega}} \mathbf{u}_{\Lambda}(z) e^{i(\mathbf{q} \cdot \mathbf{r} - \Omega t)} b_{\Lambda} + \text{H.c.}, \quad (4)$$

where  $b_{\Lambda}$  is a bosonic annihilation operator and  $\rho_M \simeq 7860 \text{ kg/m}^3$ .<sup>10</sup> The noninteracting phonon Hamiltonian is

$$H_p = \sum_{\Lambda} \Omega_{\Lambda} (b_{\Lambda}^{\dagger} b_{\Lambda} + 1/2). \quad (5)$$

The orthonormal eigenmodes  $\mathbf{u}_{\Lambda}(z)$  describe linear combinations of  $e^{\pm i k_{l,t} z}$  waves, where

$$k_{l,t} = \sqrt{(\Omega/c_{l,t})^2 - q^2}. \quad (6)$$

First, the horizontal shear mode,  $\lambda = H$ , with  $\mathbf{u}_H \parallel \hat{e}_z \times \hat{e}_q$  (where  $\hat{e}_q = \mathbf{q}/q$ ) decouples from all other modes and does not generate a deformation potential; hence it is not discussed further. The remaining modes are given by

$$\mathbf{u}(z) = \left( i q \phi_l - \frac{d\phi_l}{dz} \right) \hat{e}_q + \left( \frac{d\phi_l}{dz} + i q \phi_l \right) \hat{e}_z, \quad (7)$$

$$\phi_{l,t} = \frac{1}{\sqrt{2\pi \Omega k_{l,t}}} (a_{l,t} e^{-i k_{l,t} z} + b_{l,t} e^{i k_{l,t} z}).$$

The incoming longitudinal mode,  $\lambda = L$ , with  $a_l = 1$  and  $a_t = 0$ , exists for  $\Omega > c_l q$  with real  $k_{l,t} > 0$ . The eigenstate  $\phi_{l,t}^{(L)}$  has  $b_l = -A$  and  $b_t = B$ , where

$$A = \frac{(q^2 - k_t^2)^2 - 4q^2 k_l k_t}{(q^2 - k_t^2)^2 + 4q^2 k_l k_t}, \quad B = \frac{4q(q^2 - k_t^2) \sqrt{k_l k_t}}{(q^2 - k_t^2)^2 + 4q^2 k_l k_t}.$$

The incoming transverse mode,  $\lambda = T$ , with  $a_l = 0$  and  $a_t = 1$ , exists for  $\Omega > c_t q$ . The eigenstate  $\phi_{l,t}^{(T)}$  has  $b_l = -B$  and  $b_t = -A$ . (For  $c_t q < \Omega < c_l q$ , we have  $k_l = i |k_l|$ .) Finally, the energetically lowest solution is the Rayleigh surface wave,  $\lambda = R$ , where  $a_l = a_t = 0$  and  $k_{l,t} = i \kappa_{l,t} q$ . Here the dispersion relation is linear,  $\Omega = c_R q$  with surface velocity  $c_R = \xi c_t$ , i.e.,

$\Omega$  is not a free parameter in  $\Lambda$  anymore. Putting  $\gamma = (c_t/c_l)^2$ , we find

$$\xi = \left\{ \frac{8}{3} - \frac{4\sqrt{12\gamma - 2}}{3} \cos \left[ \frac{1}{3} \cos^{-1} \left( \frac{17 - 45\gamma}{(12\gamma - 2)^{3/2}} \right) \right] \right\}^{1/2}.$$

With  $\kappa_l = \sqrt{1 - \gamma \xi^2}$  and  $\kappa_t = \sqrt{1 - \xi^2}$ , we obtain

$$\phi_l^{(R)} = \sqrt{\frac{C}{q}} e^{-\kappa_l q z}, \quad \phi_t^{(R)} = -\sqrt{\frac{C}{q}} \frac{2i \kappa_l}{1 + \kappa_t^2} e^{-\kappa_t q z}, \quad (8)$$

$$C^{-1} = \kappa_l - \kappa_t + \frac{(\kappa_l - \kappa_t)^2}{2\kappa_l^2 \kappa_t}.$$

Using the above values for  $c_{l,t}$  we find  $\xi \simeq 0.92$ ,  $\kappa_l \simeq 0.85$ ,  $\kappa_t \simeq 0.39$ , and  $C \simeq 1.20$ .

### III. ELECTRON-PHONON COUPLING

The deformation potential couples the local electron density to  $\nabla \cdot \mathbf{U}(\mathbf{r}, z)$ , with a coupling constant  $\alpha$ . Reference 11 gives the estimate  $\alpha \approx 35 \text{ eV}$ . This yields the second-quantized interaction Hamiltonian

$$H_{ep} = \frac{\alpha}{\sqrt{\mathcal{A}}} \sum_{q\Omega\lambda} M_{q\Omega}^{(\lambda)} b_{q\Omega\lambda} \sum_{kss'} c_{k+q,s}^{\dagger} X_{kq,ss'} c_{ks'} + \text{H.c.}, \quad (9)$$

where  $U_{\mathbf{k}}$  in Eq. (3) defines the matrix

$$X_{kq} = U_{k+q} U_{\mathbf{k}}^{\dagger}. \quad (10)$$

For the Rayleigh mode, the sum over  $\Omega$  should be omitted with the replacement  $\Omega = c_R q$ . With  $\phi_l^{(\lambda)}$  specified in Eqs. (7) and (8), we obtain the  $\hat{e}_q$ -independent electron-phonon coupling matrix elements

$$M_{q\Omega}^{(\lambda)} = -\frac{(\Omega/c_l)^2}{\sqrt{2\rho_M \Omega}} \int_0^{\infty} dz |\chi(z)|^2 \phi_l^{(\lambda)}(z), \quad (11)$$

with the electronic surface state  $\chi$  in Eq. (1). For  $q \ll \text{Re}(\eta_-)$ , the overlap integral above reduces to  $\phi_l^{(\lambda)}(z = 0)$ . In what follows, we discuss physical consequences obtained from the Hamiltonian

$$H = H_e + H_p + H_{ep}. \quad (12)$$

In the concrete examples below, the chemical potential is  $\mu = v_F k_F = 0.05 \text{ eV}$ , corresponding to the BG temperature  $T_{\text{BG}} = 2k_F c_R / k_B = 3.9 \text{ K}$  and the Fermi temperature  $T_F = 580 \text{ K}$ .

### IV. LIFETIME BROADENING

We begin with the self-energy  $\Sigma_s(\mathbf{k}, \omega)$  for a helical eigenstate  $s = \pm$ . Following standard arguments,<sup>18,19</sup> the main contribution is captured to lowest nontrivial order in  $H_{ep}$ . Noting that the ‘‘tadpole’’ diagram vanishes identically, the ‘‘rainbow’’ diagram<sup>18</sup> yields independent contributions from each mode  $\lambda$ ,

$$\Sigma_s^{(\lambda)}(\mathbf{k}, \omega) = \sum_{s', v = \pm} \alpha^2 \int_0^{\infty} d\Omega \int \frac{d^2 \mathbf{q}}{(2\pi)^2} |M_{q\Omega}^{(\lambda)} X_{kq,ss'}|^2 \times \frac{v [n_B(v\Omega) + n_F(\epsilon_{\mathbf{k}+\mathbf{q},s'})]}{\omega + i0^+ + v\Omega - \epsilon_{\mathbf{k}+\mathbf{q},s'}}, \quad (13)$$

where  $n_B$  ( $n_F$ ) is the Bose (Fermi) function. For the  $R$  mode, the  $q$  integral has to include the additional factor  $\delta(\Omega - c_R q)$ , while for  $\lambda = L, T$ , we have the respective constraint  $q < \Omega/c_{l,t}$ . The decay rate  $\Gamma^{(\lambda)} = -2 \text{Im} \Sigma^{(\lambda)}$  describing lifetime broadening is then given by

$$\Gamma_s^{(\lambda)}(\mathbf{k}, \omega) = \sum_{\nu=\pm} \alpha^2 \int_0^\infty d\Omega F_{ks,\omega}^{(\lambda,\nu)}(\Omega) \times [n_B(\Omega) + n_F(\Omega + \nu\omega)]. \quad (14)$$

Here the Eliashberg function<sup>18</sup> is defined as

$$F_{ks,\omega}^{(\lambda,\pm)}(\Omega) = \sum_{s'} \int \frac{d^2\mathbf{q}}{2\pi} |M_{q\Omega}^{(\lambda)} X_{kq,ss'}|^2 \delta(\omega \pm \Omega - \epsilon_{k+q,s'}), \quad (15)$$

which represents a phonon density of states weighted by the coupling matrix elements. Performing the angular integration yields the result

$$F_{ks,\omega}^{(\lambda,\nu)}(\Omega) = \frac{1}{2\pi v_F k} \int_{q_-}^{q_+} q dq |M_{q\Omega}^{(\lambda)}|^2 \left( \frac{q_+^2 - q^2}{q^2 - q_-^2} \right)^{s'/2}, \quad (16)$$

$$q_\pm = \left| \frac{|\mu + \omega + \nu\Omega|}{v_F} \pm k \right|,$$

where  $s' \equiv s \text{sgn}(\mu + \omega + \nu\Omega)$ .

For a discussion of the lifetime, we now consider the on-shell case,  $\omega = \epsilon_{ks}$ . For the Rayleigh mode with  $c_R \ll v_F$ , we find  $s' = +$ ,  $q_+ \simeq 2k$ , and  $q_- = 0$ , yielding for both  $\nu = \pm$  the analytical result

$$F_k^{(R)}(\Omega) = \frac{C}{2\pi} \frac{\Omega^2 \sqrt{1 - (\Omega/2c_R k)^2}}{\rho_M v_F c_l^4} \Theta(2kc_R - \Omega), \quad (17)$$

with the Heaviside function  $\Theta$ . The Eliashberg functions for the other two phonon modes have to be computed numerically. Together with Eq. (17), they are shown in Fig. 1. Numerically, after a rescaling we find almost *universal* behavior in the sense

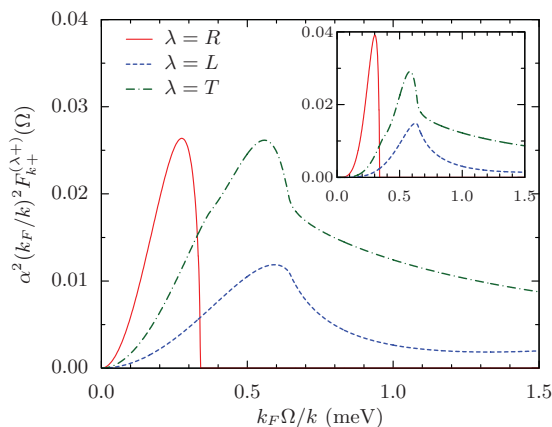


FIG. 1. (Color online) Low-frequency behavior of the Eliashberg functions  $F_{k+}^{(\lambda,+)}(\Omega)$  for the three relevant acoustic phonon modes ( $k = 0.1k_F$ ). In the rescaled units used here, the functions are approximately  $k$  independent. Inset: Same for the “transport” Eliashberg function  $\mathcal{F}$  (see main text).

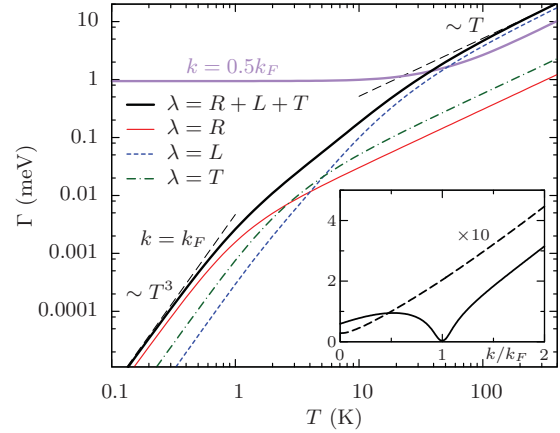


FIG. 2. (Color online) Main panel:  $T$  dependence of the decay rate  $\Gamma$  for  $k = k_F$  and for  $k = 0.5k_F$ . For  $k = 0.5k_F$ , only the  $L$  mode gives significant contributions. Inset:  $k$  dependence of  $\Gamma$  for  $T = 3.9$  K (solid line) and for  $T = 392$  K (dashed line; the shown result has to be multiplied by 10).

that the functions

$$(k_F/k)^2 F_{ks}^{(\lambda,\nu)}(k\Omega/k_F) \quad (18)$$

are essentially independent of  $k$ . The  $\Omega \rightarrow 0$  behavior is dominated by the Rayleigh mode with  $F(\Omega) \sim \Omega^2$ , but at higher energy scales (in particular, outside the regime shown in Fig. 1), the two other modes are much more important.

The resulting quasiparticle decay rate  $\Gamma_k(T)$  then follows from Eq. (14) and is shown in Fig. 2. The decay rate is dominated by the  $L$  mode except for very low energy scales, i.e., when the particle is near the Fermi surface,  $k \approx k_F$ , and temperature is low,  $T \lesssim T_{BG}$ . For high temperatures, when  $k_B T$  is higher than the maximum phonon energy, Eq. (14) predicts a characteristic  $\Gamma \sim T$  law, which allows one to identify electron-phonon scattering processes in practice. More precisely, the slope is determined by the effective electron-phonon coupling parameter  $\Gamma_k = 2\pi\lambda_k k_B T$ , where

$$\lambda_k = \frac{1}{2\pi} \sum_{\lambda,\nu=\pm} \alpha^2 \int_0^\infty d\Omega \frac{F_k^{(\lambda,\nu)}(\Omega)}{\Omega}. \quad (19)$$

At the Fermi surface, we find  $\lambda_{k_F} \simeq 0.13$  with the main contribution coming from the  $L$  mode.

For  $k = k_F$  and  $T \ll T_{BG}$ , the decay rate is dominated by the  $R$  mode, and we obtain

$$\Gamma_{k_F}(T) = \frac{28\zeta(3)C}{\pi} \frac{\alpha^2 c_R^3 k_F^3}{\rho_M v_F c_l^4} \left( \frac{T}{T_{BG}} \right)^3, \quad (20)$$

with  $\zeta(3) \simeq 1.202$ .<sup>26</sup> This  $T^3$  law and the crossover to the linear  $T$  dependence for  $T \gg T_{BG}$  are shown in Fig. 2. We note that away from the Fermi surface, the  $T = 0$  decay rate stays finite and scales as  $\Gamma_k \sim |k - k_F|^3$  for  $k \rightarrow k_F$ .

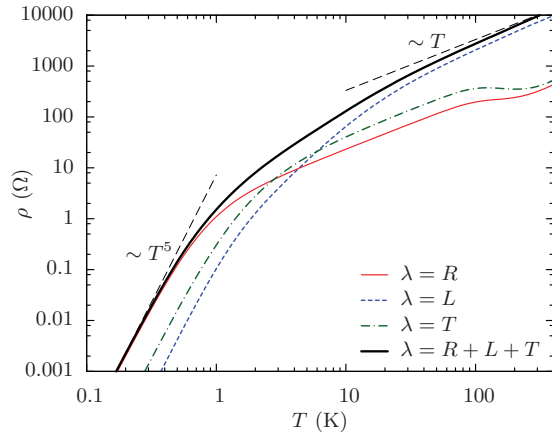


FIG. 3. (Color online) Temperature dependence of the phonon contribution to the surface resistivity. Note the double-logarithmic scales. Individual contributions of each phonon mode are also shown.

## V. RESISTIVITY

Next we compute the phonon contribution to the resistivity,  $\rho$ , using a quasiclassical Boltzmann transport theory as employed recently for graphene,<sup>14,15</sup>

$$\rho = \frac{2}{e^2 v_F^2} \frac{1}{D(\mu)} \frac{1}{\langle \tau \rangle}, \quad \langle \tau \rangle = \frac{\int d\epsilon (-\partial_\epsilon n_F) D(\mu + \epsilon) \tau(\epsilon)}{\int d\epsilon (-\partial_\epsilon n_F) D(\mu + \epsilon)}, \quad (21)$$

with the density of states  $D(E) = |E|/(2\pi v_F^2)$ . This approach is valid for  $|\mu| \langle \tau \rangle \gg 1$ , which is equivalent to  $G_Q \rho \ll 1$  with the conductance quantum  $G_Q = e^2/h$ . Under the Born approximation, the inverse of the energy-dependent electron-phonon transport scattering time  $\tau(\epsilon_{ks})$  separates into independent phonon mode contributions,  $1/\tau = \sum_\lambda 1/\tau^{(\lambda)}$ , with

$$\frac{1}{\tau^{(\lambda)}(\epsilon_{ks})} = \sum_{q,s'} (1 - \cos \theta_{k,q}) W_{k,s \rightarrow k+q,s'}^{(\lambda)} \frac{1 - n_F(\epsilon_{k+q,s'})}{1 - n_F(\epsilon_{ks})}, \quad (22)$$

where  $\theta_{k,q} = \theta_{k+q} - \theta_k$  is the angle between  $\mathbf{k}$  and  $\mathbf{k} + \mathbf{q}$ . Fermi's golden rule yields the transition probability

$$W_{k,s \rightarrow k+q,s'}^{(\lambda)} = \frac{2\pi}{\mathcal{A}} \sum_{v=\pm} \alpha^2 \int_0^\infty d\Omega |M_{q\Omega}^{(\lambda)} X_{kq,ss'}|^2 \times v n_B(v\Omega) \delta(\epsilon_{ks} + v\Omega - \epsilon_{k+q,s'}). \quad (23)$$

The result can again be expressed using a transport Eliashberg function  $\mathcal{F}_{ks}^{(\lambda,\pm)}(\Omega)$  given by Eq. (15) with  $\omega = \epsilon_{ks}$  and an additional factor  $(1 - \cos \theta_{k,q})$  in the integral. After the angular integration, we obtain  $\mathcal{F}$  as in Eq. (16) but with an

additional factor  $(q^2 - q_-^2)/[2k(q_+ - k)]$  in the integrand. The resulting functions are depicted in the inset of Fig. 1. After some algebra, we arrive at<sup>27</sup>

$$\frac{1}{\tau(\epsilon_{ks})} = \sum_{\lambda,v=\pm} \alpha^2 \int_0^\infty d\Omega \mathcal{F}_{ks}^{(\lambda,v)}(\Omega) \times v n_B(v\Omega) \frac{1 - n_F(\epsilon_{ks} + v\Omega)}{1 - n_F(\epsilon_{ks})}. \quad (24)$$

In Fig. 3, we show the full  $T$  dependence of the phonon-induced resistivity  $\rho$ . For  $T \ll T_{BG}$ , the resistivity is dominated by the  $\Omega \rightarrow 0$  behavior of  $\mathcal{F}(\Omega)$ . The latter comes from the  $R$  mode with  $\mathcal{F} \sim \Omega^4$ , which implies  $\rho \sim T^5$  as  $T \rightarrow 0$ . The prefactor can be evaluated exactly,

$$G_Q \rho(T \rightarrow 0) = \frac{1488 \zeta(5) C}{\pi} \frac{\alpha^2 c_R^3 k_F^2}{\rho_M v_F^2 c_l^4} \left( \frac{T}{T_{BG}} \right)^5, \quad (25)$$

where  $\zeta(5) \simeq 1.037$ .<sup>26</sup> We thus recover the standard BG power law,  $\rho \sim T^5$ , as in bulk three-dimensional metals,<sup>28</sup> which is here caused by the coupling to the Rayleigh surface phonon mode. For  $T \gg T_{BG}$ , on the other hand, we find a  $\rho \sim T$  law predominantly due to the  $L$  mode. For  $T \approx T_{BG}$ , all three phonon modes are important.

## VI. CONCLUSIONS

We have formulated an analytically tractable effective low-energy theory of the surface Dirac fermion state in a strong TI with deformation-potential coupling to acoustic phonons. The influence of phonons could be observed as the characteristic temperature-dependent decay rate  $\Gamma$  of quasiparticles in ARPES, or from their  $T$ -dependent contribution to the surface resistivity. The phonon-mediated effective interaction among surface fermions can also be attractive at low frequencies, possibly allowing for superconducting correlations; however, this topic as well as studies of the electron-induced modification of phonon properties in this system or the physics near the Dirac point ( $k_F = 0$ ) are left for future work. We hope that our predictions will soon be tested experimentally.

*Note added:* Recently, we became aware of an experimental investigation of electron-phonon scattering for the topological state of  $\text{Bi}_2\text{Se}_3$ .<sup>29</sup> In particular, the order of magnitude for the measured electron-phonon coupling strength,  $\lambda = 0.25(5)$ , is in excellent agreement with our prediction for  $\text{Bi}_2\text{Te}_3$ .

## ACKNOWLEDGMENTS

This work was supported by the Humboldt foundation and by the SFB TR 12 of the DFG.

<sup>1</sup>M. Z. Hasan and C. L. Kane, *Rev. Mod. Phys.* **82**, 3045 (2010).

<sup>2</sup>X. L. Qi and S. C. Zhang, e-print arXiv:1008.2026.

<sup>3</sup>L. Fu and C. L. Kane, *Phys. Rev. B* **76**, 045302 (2007).

<sup>4</sup>X. L. Qi, T. L. Hughes, and S. C. Zhang, *Phys. Rev. B* **78**, 195424 (2008).

<sup>5</sup>D. Hsieh, Y. Xia, D. Qian, L. Wray, J. H. Dil, F. Meier, J. Osterwalder, L. Patthey, J. G. Checkelsky, N. P. Ong, A. V. Fedorov, H. Lin, A. Bansil, D. Grauer, Y. S. Hor, R. J. Cava, and M. Z. Hasan, *Nature (London)* **460**, 1101 (2009); Y. L. Chen, J.-H. Chu, J. G. Analytis, Z. K. Liu, K. Igarashi, H.-H. Kuo, X. L. Qi, S. K. Mo, R.

- G. Moore, D. H. Lu, M. Hashimoto, T. Sasagawa, S. C. Zhang, I. R. Fisher, Z. Hussain, and Z. X. Shen, *Science* **329**, 659 (2010); L. A. Wray, S.-Y. Xu, Y. Xia, Y. S. Hor, D. Qian, A. V. Fedorov, H. Lin, A. Bansil, R. J. Cava, and M. Z. Hasan, *Nat. Phys.* **6**, 855 (2010).
- <sup>6</sup>N. P. Butch, K. Kirshenbaum, P. Syers, A. B. Sushkov, G. S. Jenkins, H. D. Drew, and J. Paglione, *Phys. Rev. B* **81**, 241301(R) (2010).
- <sup>7</sup>D. X. Qu, Y. S. Hor, J. Xiong, R. J. Cava, and N. P. Ong, *Science* **329**, 821 (2010).
- <sup>8</sup>J. G. Analytis, R. D. McDonald, S. C. Riggs, J.-H. Chu, G. S. Boebinger, and I. R. Fisher, *Nat. Phys.* **6**, 960 (2010).
- <sup>9</sup>W. Richter, H. Köhler, and C. R. Becker, *Phys. Status Solidi B* **84**, 619 (1977).
- <sup>10</sup>J. O. Jenkins, J. A. Rayne, and R. W. Ure Jr., *Phys. Rev. B* **5**, 3171 (1972).
- <sup>11</sup>B. L. Huang and M. Kaviani, *Phys. Rev. B* **77**, 125209 (2008).
- <sup>12</sup>K. M. F. Shahil, M. Z. Hossain, D. Teweldebrhan, and A. A. Balandin, *Appl. Phys. Lett.* **96**, 153103 (2010); J. Qi, X. Chen, W. Yu, P. Cadden Zimansky, D. Smirnov, N. H. Tolk, I. Miotkowski, H. Cao, Y. P. Chen, Y. Wu, S. Qiao, and Z. Jiang, *ibid.* **97**, 182102 (2010).
- <sup>13</sup>Ph. Hofmann, *Prog. Surf. Sci.* **81**, 191 (2006).
- <sup>14</sup>E. H. Hwang and S. Das Sarma, *Phys. Rev. B* **77**, 115449 (2008).
- <sup>15</sup>E. Mariani and F. von Oppen, *Phys. Rev. B* **82**, 195403 (2010).
- <sup>16</sup>D. K. Efetov and P. Kim, *Phys. Rev. Lett.* **105**, 256805 (2010).
- <sup>17</sup>A. Knäbchen, *Phys. Rev. B* **55**, 6701 (1997).
- <sup>18</sup>B. Hellsing, A. Eiguren, and E. V. Chulkov, *J. Phys.: Condens. Matter* **14**, 5959 (2002).
- <sup>19</sup>P. M. Echenique, R. Berndt, E. V. Chuklov, Th. Fauster, A. Goldmann, and U. Höfer, *Surf. Sci. Rep.* **52**, 219 (2004).
- <sup>20</sup>S. R. Park, W. S. Jung, C. Kim, D. J. Song, C. Kim, S. Kimura, K. D. Lee, and N. Hur, *Phys. Rev. B* **81**, 041405(R) (2010).
- <sup>21</sup>L. D. Landau and E. M. Lifshitz, *Elasticity Theory* (Pergamon, New York, 1986), Chap. 24.
- <sup>22</sup>Y. M. Sirenko, K. W. Kim, and M. A. Stroschio, *Phys. Rev. B* **56**, 15770 (1997).
- <sup>23</sup>For a phenomenological discussion of a different electron-phonon coupling mechanism in the context of surface acoustic waves, see P. Thalmeier, *Phys. Rev. B* **83**, 125314 (2011).
- <sup>24</sup>C. X. Liu, X. L. Qi, H. J. Zhang, X. Dai, Z. Fang, and S. C. Zhang, *Phys. Rev. B* **82**, 045122 (2010).
- <sup>25</sup>H. Zhang, C. X. Liu, X. L. Qi, X. Dai, Z. Fang, and S. C. Zhang, *Nat. Phys.* **5**, 438 (2009).
- <sup>26</sup>M. Abramowitz and I. A. Stegun, *Handbook of Mathematical Functions* (Dover, New York, 1971).
- <sup>27</sup>Equation (24) ignores screening by the surface charge carriers themselves. Note that this approximation is consistent with experimental results in graphene (Ref. 16).
- <sup>28</sup>N. W. Ashcroft and N. D. Mermin, *Solid State Physics* (Saunders College, Philadelphia, 1976).
- <sup>29</sup>R. C. Hatch, M. Bianchi, D. Guan, S. Bao, J. Mi, B. B. Iversen, L. Nilsson, L. Hornekaer, and P. Hofmann, *Phys. Rev. B* **83**, 241303(R) (2011).